Applied Energy 118 (2014) 166–172

Contents lists available at ScienceDirect

Applied Energy

journal homepage: www.elsevier.com/locate/apenergy

Accurate simulation of thermoelectric power generating systems

Andrea Montecucco *, Andrew R. Knox

School of Engineering, College of Science and Engineering, University of Glasgow, UK

HIGHLIGHTS

- We model the thermal and electrical dynamics of thermoelectric power generating systems.
- Both transient and steady-state conditions are considered.
- We develop a computer program for transient simulations of thermoelectric systems.
- The program simulates the electro-thermal coupled effects that occur during changes in the operating conditions.
- Comparison of experimental and simulation results shows great accuracy.

ARTICLE INFO

Article history:
Received 9 October 2013
Received in revised form 14 December 2013
Accepted 18 December 2013
Available online 14 January 2014

Keywords:
Thermoelectric
TEG
Heat transfer
Computer simulation
Peltier
Seebeck

ABSTRACT

Recent interest in the use of thermoelectric generators (TEGs) to recover waste heat in large-scale applications calls for precise simulation to appropriately design complicated and dynamic systems. The aim of this work is to develop a computer tool to accurately simulate the thermal and electrical dynamics of a real thermoelectric (TE) power generating system.

The computer-aided model presented here is able to accurately simulate the non-linear electro-thermal coupled effects which occur during changes in the operating conditions, e.g. temperature or load changes.

Simulation results are compared to experimental data obtained from a real TE system. The comparison shows great accuracy both during transients and in the steady-state, thus validating the model as a reliable tool to simulate TE generating systems.

1. Introduction

Thermoelectric (TE) devices can directly convert thermal energy into electrical energy and vice versa. Thermoelectricity, based on the fact that charge carriers can be set in motion by a difference of temperature, generally refers to two main physical phenomena: the Seebeck effect and the Peltier effect. The former states that a certain open-circuit voltage is created in a material kept between two different temperatures. The Seebeck coefficient α (V/K) is a material property that relates the open-circuit thermoelectric potential V_{OC} (V) with the temperature difference ΔT (K), or

$$V_{OC} = \alpha \Delta T \tag{1}$$

The Peltier effect states that a direct current I(A) passing through a circuit of dissimilar materials pumps thermal power from one material to the other:

$$P_P = \pi I = \alpha I T_j \tag{2}$$

where π (V) is the Peltier coefficient and the last equivalence comes from the Kelvin relationship; T_j is the junction temperature.

Other important phenomena occurring in thermoelectric devices are the well-known Joule heating and the Thomson effect. The latter states that there is reversible absorption or liberation of heat (in excess of the joule dissipation I^2R) in a homogeneous material simultaneously exposed to temperature gradient and electric current:

$$P_T = \tau I \Delta T \tag{3}$$

where τ (V/K) is the Thomson coefficient, defined as

$$\tau = T_{AVG} \frac{d\alpha}{dT} \tag{4}$$

The Thomson effect is usually much smaller than the Joule heating [1,2] and ts contribute can be significant under large temperature differences [3,4]; also, the Thomson coefficient is difficult to obtain experimentally, therefore it is often neglected in literature. Its effect is not included in this article.

Doped semiconductors prove to be the materials with the best thermoelectric properties. Multiple pellets of *p*- and

* Corresponding author. Tel.: +44 1413302768.
E-mail address: andrea.montecucco@glasgow.ac.uk (A. Montecucco).

0306-2619/$ - see front matter © 2013 Elsevier Ltd. All rights reserved.
http://dx.doi.org/10.1016/j.apenergy.2013.12.028

n-semiconductor are connected electrically in series and thermally in parallel to achieve and/or sustain higher voltages, thus forming a TE module. This paper will focus on TE generators (TEGs); Fig. 1 shows a 3D model of a TEG module where thermal energy is applied on the bottom ("hot" side). The pellets are electrically series-connected by solder and an Aluminium-based ceramic layer serves as electrical isolation and mechanical substrate. The resulting module is quite robust and reliable, and operates without any vibration or noise. It is commercially produced in a wide range of sizes from a few millimetres to several centimetres on a side. Multiple modules can be electrically connected in series or parallel in order to achieve higher output voltages and currents. Heat is conducted through the module while additional heat is generated (Joule) inside the module and pumped (Peltier) through the hot and cold sides as described by the coloured arrows. In TE power generation the Peltier effect is parasitic because it reduces the temperature difference across the device, thus increasing the module's effective thermal conductivity. Thermoelectric heat pumps (coolers or heaters) have been used for many years in applications ranging from IC microcoolers, to refrigerators [5], to power stations [6], and they are often referred to as Peltier devices. Due to their low efficiency, often less than 5%, thermoelectric generators have on the contrary been used predominantly in military and aerospace projects or for applications in which cost is not as important as the ability to reliably generate power in hostile or maintenance-free environments. However, interest in TEGs has recently increased because of concerns about climate change, coupled with increasing performance and lower module cost. TEGs can effectively lend themselves to sustainable applications of waste heat recovery in which thermal energy is rejected to ambient and is effectively free, e.g. in vehicles [7–10] and stoves [11,12]. TEGs can also be used to harvest geothermal energy [13] or combined to PV, solar thermal or thermophotovoltaic systems [14–16]. Moreover, recent advances in TE materials and 'mass-production' volumes [17,18] will continue to lead to a further improvement of TEGs' efficiency and reduction of their cost, respectively.

It is of fundamental importance to carefully design large-scale systems in which materials cost is of great relevance. However TE systems are usually composed of heat masses, TEGs and power and control electronics and they are influenced by several thermal and electronic phenomena whose interaction is complex. Moreover TEGs are often employed in dynamic environments which frequently undergo thermal transients. Actual CAD tools do not yet include the ability to model thermoelectric effects therefore they cannot be successfully used to accurately simulate the electro-thermal coupled effects which take place during changes in the system operating conditions, e.g., temperature, power or load changes. In literature some research has focused on this issue; Lineykin and Ben-Yaakov [19] have divided the TE module into a grid of spatially discretized thermal circuits then transformed into their electrical analogies. The transient term is included in the model as a parallel electrical capacitor to take into account an additional time-related term due to the change in stored heat energy. A similar approach has been followed by Chen et al. [20]. The accuracy of the simulation is related to the number of cells used and the parameters are difficult to obtain from manufacturers' data sheets, but most importantly they do not offer a theoretical solution to the problem because their governing equations are based on steady-state solutions. A more appropriate approach would be to study the transient physical equations which describe TE devices behaviour; among these the most important is the heat equation. Al-Nimr et al. [21] have already explored this possibility but they used fixed temperatures as boundary conditions at the two sides of the TE module, assuming that those temperatures are not varying, i.e., supposing thermal isolation (or steady-state). However, during thermal transients there is exchange of heat through the sides.

Very recently two very interesting works by Cheng and Huang [22] and Meng et al. [23] proposed two models for thermoelectric coolers. The former slightly overestimates the temperature difference in steady-state, while the second has a maximum error of 4.5 K over a temperature difference of around 37 K (with a current input of 1 A).

We have already provided a mathematical solution of the one-dimensional heat conduction equation for TE devices that includes internal Joule heat generation and dynamic exchanges of heat through the hot and cold sides in [24].

The aim of this work is to couple the aforementioned solution with the other thermal and electrical phenomena occurring in real TE systems. The resulting physical model, described in Section 2, takes into account the dynamic relations between the several thermal masses and the most important thermoelectric phenomena occurring in a generalised TE system.

The physical model is then used as the basic structure to develop a computer tool, described in Section 3, capable of accurate simulations of the thermal and electrical dynamics of a physical TE power generating system. The model is created in Simulink and Matlab and a comparison between experimental and simulated

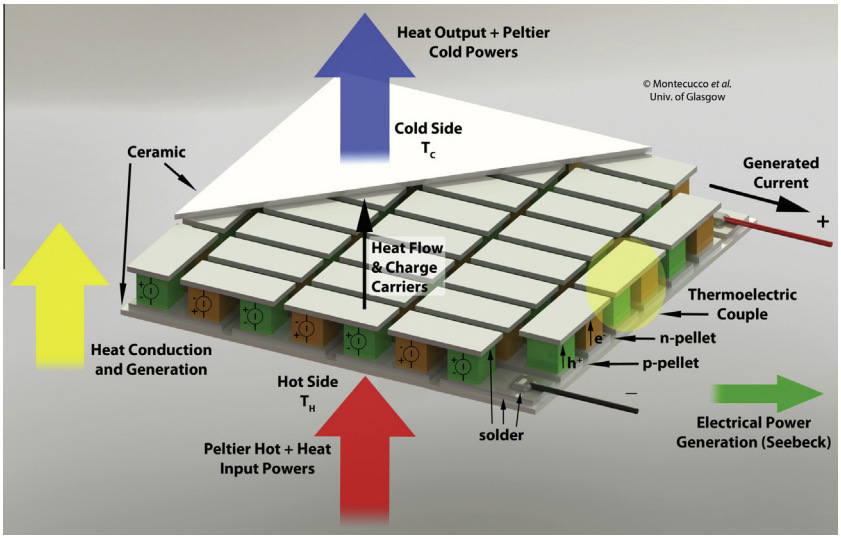

Fig. 1. 3D model of a thermoelectric generator showing the main physical effects.

results is presented in Section 4 to demonstrate the effectiveness and accuracy of the proposed simulation model.

2. Generic model of a thermoelectric system

Generally speaking, a TE system is composed of several thermal masses which store and exchange heat through conduction and/or convection. Heat is partially converted to or from electricity inside the TE device and/or in other elements, e.g., electrical heaters. It is very important to optimally design the thermal interconnection of the TE device with the rest of the system to guarantee optimal performance [25]. This paper ultimately aims at developing a model that can be used to aid TE system design.

Fig. 2 shows the architecture of a generic TE power generating system. The TEG is usually in contact with a thermal mass on both the hot and cold side. Power is provided to or removed from the thermal masses in the form of electrical or heat power, leading to changes in the thermal energy stored inside the thermal masses. Through conduction or convection part of this energy is transferred to and from the TEG module. The TEG is modelled considering the sides of the TEG separately from the inner part. The heat equation (HE) deals with both the heat conduction and generation (Joule heating) inside the TEG. Additional heat is pumped at the sides where there is a junction of two dissimilar materials (Peltier effect).

Part of the energy flowing through the TEG is converted into electrical power and the process is closely related to the thermoelectric effects described by the Eqs. (1) and (2).

Conduction and convection equations provide the rate of thermal energy flowing from one medium to the other in time. The thermal conduction equation (Fourier's law) is written in time-derivative form as:

$$\frac{dE_{cond}}{dt} = -\kappa A \frac{dT}{dx} \tag{5}$$

where E_{cond} (J) is the thermal energy, κ (W/mK) is the thermal conduction coefficient, A (m^2) is the surface of heat exchange and x (m) is the direction of heat transfer, perpendicular to A. The heat convection equation is

$$\frac{dE_{conv}}{dt} = hA\Delta T(t) \tag{6}$$

where h(W/m^2 K) is the heat convection coefficient and $\Delta T(t) = T(t) - T_\infty$ is time-dependent.

Any lumped thermal mass changes its temperature when receiving or losing thermal energy:

$$E_{therm} = mC\Delta T(t) \tag{7}$$

where mC (J/K) is the heat capacity of the thermal mass, which defines its ability to keep heat energy.

As indicated in Fig. 2, $T_{\infty H}$ is used in this paper for the temperature of the hot thermal mass and T_H is the temperature on the hot side of the TEG, while $T_{\infty C}$ and T_C are the temperatures of the cold thermal mass and TEG cold side respectively.

3. Computer model

The solution to the heat equation (HE) presented in [24] was programmed in Matlab, therefore the Mathworks suite was chosen to develop the simulation program. The model includes several blocks and performs time-step simulations. Simulink is an excellent choice of environment for this task.

Section 3.2 presents the heat equation block, Section 3.3 deals with the thermal part and 3.4 explains the electrical part of the system.

3.1. System architecture

Fig. 3 shows the architecture of the Simulink model developed in this work which will be described shortly.

The HE computes the transient solution starting from an initial condition of T_C and T_H, and with constant values for $T_{\infty H}, T_{\infty C}$ and the load current I_{load}. It can provide the temperature distribution inside the TE device at any instant in time, even if for this model, at system level, we are interested in the temperatures only at the hot and cold sides of the TEG module. The HE allows the side temperatures T_H and T_C to change depending on the temperatures $T_{\infty H}$ and $T_{\infty C}$ of the thermal masses in contact with the TEG through conduction or convection media. The temperature difference across these media changes dynamically, thanks to the Newton's Law of Cooling, as already described in [24].

In the solution of the HE the temperatures of the thermal masses $T_{\infty H,C}$ are considered constant; however, in a real system during a transient they vary depending on the energy added or removed by P_{in} and P_{out}. Similarly, the temperatures at the sides of the TEG are influenced also by the actual load current which in turn determines the value of the Peltier effect (see Eq. 2). This is why in Fig. 3 the 'HE Block' is connected to both to the 'Electrical Block' and to the 'Thermal Block'. The thermal block requires α and I_{load} form the electrical block to deal with Peltier effect. The transient evolution of the temperature difference across the TEG device and the system's dynamic exchange of heat due to P_{in} and P_{out} continuously influence the temperatures in the whole system.

Therefore in order to couple the continuous-time transient solution provided by the HE to the temperatures' evolution in

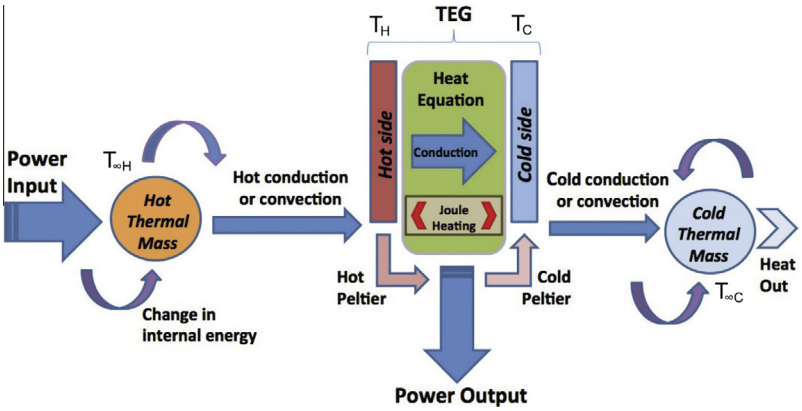

Fig. 2. Architecture of a thermoelectric power generating system.

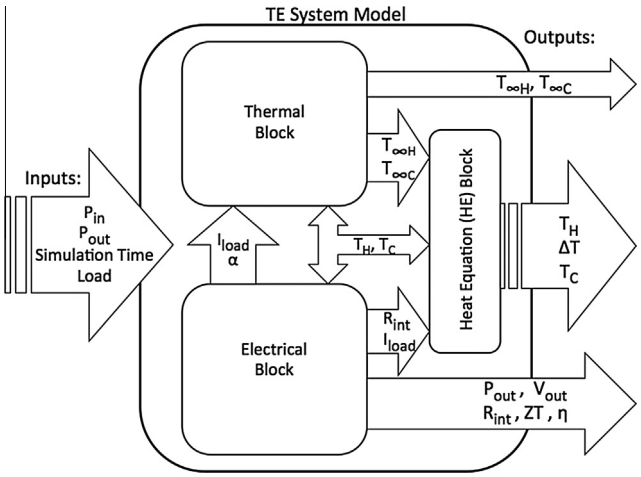

Fig. 3. Block architecture of the presented model. The inputs to the different blocks are written inside the arrows.

the remaining parts of the system (thermal masses, input/output thermal energy and electrical load), the model is designed in the discrete-time domain. Within each time step of duration t_{step} (s) the HE computes the dynamics inside the TEG for a transient of duration t_{step}. The temperatures in the remaining parts of the system change as described by Eqs. (5)–(7), in which the derivative term is substituted by slope terms. This direct examination in discrete terms aids the comprehension of the underlying physical effects in the system.

To understand how the model is structured, let's consider two successive time steps, corresponding at two program's discrete iterations, called i and $i+1$. It must be noted that the calculations made during each iteration are computed directly using the equations provided in this paper, without any trial-and-error or iterative method. During the iteration i the heat equation uses the electrical parameters and the heat masses' temperatures $T_{\infty H(i)}$ and $T_{\infty C(i)}$, considered constant during t_{step}, and the hot and cold side temperatures $T_{H(i)}$ and $T_{C(i)}$ as initial values; it computes the values of $T_{H(i+1)}$ and $T_{C(i+1)}$ corresponding to their evolution after the transient time t_{step} and outputs them through a memory block of duration t_{step}, so that they are actually available only at the start of iteration $i+1$. The HE block is described in Section 3.2. At iteration i the model also updates the temperatures of the thermal masses depending on the quantity of heat energy provided by P_{in} and P_{out} during t_{step}, so that they are ready for iteration $i+1$. The equations used to update these temperatures are described in the Section 3.3.

3.2. The TEG heat equation block

The solution to the HE provided in [24] treats the TEG module as a whole block, i.e. it does not deal with the different materials (ceramic, semiconductor, solder) separately; it also does not divide the semiconductor materials into single pellets or thermocouples. This is done by design because the parameters for the model are obtained only from the physical dimensions of the module and from its direct use in the system, i.e. by representing a real system.

The HE code is programmed into a Matlab embedded equation block. The input variables to the block are:

- TEG geometrical parameters: surface A and thickness L.
- Conduction and convection coefficients: open-circuit thermal conductivity k and thermal diffusivity coefficient $\epsilon = \frac{thermal\ conductivity\ k}{volumetric\ heat\ capacity\ \rho C_p}$ of the TEG; thermal transfer coefficients through the hot and cold mediums β_H and β_C.
- Electrical parameters of the TEG: internal resistance R_{int} and current I_{load}.
- Temperatures at the beginning of the iteration: $T_{\infty H}, T_{\infty C}, T_H$ and T_C.
- Time step duration t_{step}.

β_C and β_H may vary if the materials in contact with the cold and hot sides change properties, e.g. increased convection. ϵ can vary with temperature, but in this model it is considered constant. The time step size t_{step} is constant and chosen based on the knowledge of the TE system; it is a compromise between the thermal time constant of the transient evolution inside the TEG and the temperature change in the thermal masses of the system. Values between 1 s and 3 s are usually chosen to satisfactorily model the physical system. For systems with a very high energy flux, e.g., large engine exhaust gas systems, values of under 1 s might be more appropriate.

$T_{\infty H}, T_{\infty H}, T_C, T_H, I_{load}, R_{int}$ are fed iteratively at the beginning of every iteration from the rest of the Simulink model.

As already explained in Section 3.1, the HE block produces two outputs, T_C and T_H, that are the temperatures on the cold and hot sides after that particular iteration cycle of duration t_{step}. T_C and T_H are then passed through a memory block so that they are effectively available only after t_{step}, i.e., at the beginning of the successive iteration. The block could be set to calculate temperatures inside the TEG too, but these are not of interest to the aim of the simulation (nor, usually, to the system designer).

If there are TEG modules connected in series or parallel some of the inputs required by the HE will be scaled accordingly depending on the total number of modules N_{tot} : $A_{tot} = N_{tot}A$, while R_{int} and I_{load} will be provided by the electrical block, as described in Section 3.4.

3.3. The thermal block

The most important tasks executed by the hot side block are the update of the temperature $T_{\infty H}$ of the hot thermal mass and the update of the TEG hot side temperature T_H, accounting for the Peltier effect.

Consider now the input power transferred to the hot thermal mass. This can be provided by an electrical heater or by thermal conduction/convection. For the electrical case it is easily measured while in the thermal case it can be calculated using the well-known laws of heat conduction or convection. As shown in Fig. 3, part of the input power goes into changing the quantity of heat energy stored in the hot thermal mass, while the remaining thermal energy is transferred (through the hot thermal mass) to the TEG. Heat losses can be accounted for in another term P_{lossH}. It can be written:

$$P_{in} = \frac{m_H C_H \Delta T_{\infty H}}{t_{step}} + h_H A \Delta T_H + P_{lossH} \tag{8}$$

where $m_H C_H$ is the hot thermal mass heat capacity J/K, $\Delta T_{\infty H}$ is the change in temperature of the hot thermal mass during t_{step}, h_H is the convection coefficient (or for conduction the conduction coefficient over the thickness) of the medium between the hot thermal mass and the TEG, A is the area of the TEG and ΔT_H is the temperature difference across the medium.

From Eq. (8) it would be possible to obtain the new value for $T_{\infty H}$, however, we first need to account for the Peltier effect which acts on the second term on the right of Eq. (8). The Peltier effect pumps additional power from the hot side to the cold side, thus effectively reducing the hot side temperature T_H provided by the HE. If we write that $P_{convH} = h_H A \Delta T_H = h_H A (T_{\infty H} - T_H)$, where T_H is the result of the HE, then we can correct the value of T_H by calculating its 'real' value:

$$T_{Hreal} = T_{\infty H} - \frac{P_{convH} + P_{PeltH}}{h_H A} \quad (9)$$

where $P_{PeltH} = \alpha I T_H$ from Eq. (2). Now that the 'real' value for T_H is obtained, from Eq. (8) it is possible to calculate $T_{\infty H}$ for the next iteration:

$$T_{\infty H(i+1)} = T_{\infty H(i)} + \frac{[P_{in} - P_{lossH} - h_H A(T_{\infty H(i)} - T_{Hreal})]t_{step}}{m_H C_H} \quad (10)$$

It can be noted that, depending on the polarity of the second term on the right of Eq. 10, $T_{\infty H(i+1)}$ can be greater or smaller than $T_{\infty H(i)}$. T_{Hreal} and $T_{\infty H(i+1)}$ will be used in the next iteration $(i+1)$ of the HE as the initial value of the hot side temperature and as the temperature of the hot thermal mass, respectively.

For the cold part of the system similar considerations hold true. The power flowing to the cold thermal mass is the sum of the thermal power flowing through the TEG and the thermal power pumped to the cold junction by the Peltier effect. In a similar way as for the hot side we update T_C to its 'real' value:

$$T_{Creal} = T_{\infty C} + \frac{h_C A(T_C - T_{\infty C}) + \alpha I T_C}{h_C A} \quad (11)$$

It is now possible to obtain $T_{\infty C(i+1)}$ as

$$T_{\infty C(i+1)} = T_{\infty C(i)} + \frac{[h_C A(T_{Creal} - T_{\infty C(i)}) - P_{out} - P_{lossC}]t_{step}}{m_C C_C} \quad (12)$$

where P_{out} is the power removed from the cold thermal mass and $P_{C_{out}}$ takes into account any thermal power lost to ambient on the cold side.

Both the values calculated in Eq. (11) and (12) are passed to the HE block for the next iteration $(i+1)$.

3.4. The electrical block

A TEG can be modelled as a voltage source V_{OC} in series with its internal resistance R_{int}, even during transients, because their electrical dynamic response is in order of nanoseconds [26]. Therefore, when the TEG is connected to a load R_{load} it can be written that the load voltage is

$$V_{load} = V_{OC} - R_{int} I_{load} \quad (13)$$

It can be noted that both the internal resistance and the open-circuit voltage can be approximated to linear functions of the temperature difference ΔT across the device [27], therefore Eq. (13) can be updated to

$$V_{load} = m_{V_{OC}} \Delta T - (m_{R_{int}} \Delta T + q_{R_{int}}) I_{load} \quad (14)$$

As stated in the Introduction, this work neglects the Thomson effect; therefore, $m_{V_{OC}}$ is considered constant and equal to the Seebeck coefficient α (V/K). $m_{R_{int}}$ (Ω/K) and $q_{R_{int}}$ (Ω) are constant coefficients, too.

In order to use Eq. 14 in the model, the appropriate values for the coefficients $m_{V_{OC}}, m_{R_{int}}$ and $q_{R_{int}}$ should be obtained through an electrical characterisation of the TEGs used in TE system [28].

The electrical block also deals with series and parallel connection of TEG modules. It is assumed that all the modules are identical and all are subjected to equal thermal conditions. If there are N_S modules in series and N_P modules in parallel, for a total of N_{tot}, the total open-circuit voltage is $V_{OCtot} = N_S V_{OC}$ and the load current I_{load} is N_P times the current in a single branch. It can then be written, from Eq. (13), that

$$V_{load} = N_S V_{OC} - \frac{N_S R_{int} I_{load}}{N_P} \quad (15)$$

The dimension-less figure of merit ZT and the actual efficiency η are also calculated [14,9]:

$$ZT = \frac{L}{R_{int} A} \frac{\alpha^2}{k} \frac{T_H + T_C}{2} \quad (16)$$

$$\eta = \frac{V_{load} I_{load}}{P_{in} - P_{lossH}} \quad (17)$$

In Eq. 16 the electrical conductivity was written as $\sigma = L/(R_{int}A)$ and the average temperature of the device as $T_{AVG} = (T_H + T_C)/2$.

The electrical part of the Simulink model computes the values of R_{int} and V_{load} depending on the actual temperature gradient ΔT and on the electrical parameters I_{load}, N_S, N_P. The Peltier term is calculated as $N_{tot} \alpha T_j I_{single}$, where I_{single} is the current passing through a single TEM. The load current (or voltage) in a real TE system is set either by a constant R_{load} connected to the TEG, or by an interfacing power electronic converter with Maximum Power Point Tracking (MPPT) [29]. For flexibility of simulation, the desired load is passed to the model as an input, but the model provides also the maximum theoretical power, i.e. when $V_{load} = V_{OC}/2$, to compare actual electrical power output with the maximum that can be extracted.

4. Experimental and simulation results

In order to test the ability of the proposed Simulink–Matlab model to simulate real TE generating systems, a transient experiment has been performed in the laboratory and then simulated by computer. The results for both and a discussion about their comparison is presented in this Section.

4.1. Experimental test rig

The TE system used in the experiment is identical to that presented in [28]. The cold thermal mass is formed of a water-cooled copper block and the hot thermal mass is a copper block containing one high-power high-temperature electrical heater powered by a DC power supply unit. The TEG output is connected to an electronic load. The TEG module is compressed between the two blocks by a mechanical fixture which does not introduce thermal shocks or short-circuit the thermal path. The mechanical compression force on the system is sensed by a load cell and thermocouples measure the temperatures of the water, the heater, and the faces of the TEG module (directly touching them). All the sensors are connected to a datalogger. Each of the electronic instruments used is connected by the IEEE-488 interface (GPIB) to a computer and controlled by a program created in the Agilent VEE Pro software.

The copper blocks have a thermal capacity of approximately 565 J/K (Copper volumetric heat capacity $C_{V_{Cu}} = 3.45$ J/cm^3 K), the thermal transfer coefficient for between the TEG and the hot and cold thermal masses are respectively 9100 and 11,800 W/m^2 K (Copper thermal conductivity $k_{Cu} = 400$ W/mK; the heater is 2.2 cm from the TEG hot side, the water pipes are 1.7 cm from the TEG cold side).

The input power is provided by electrical heaters and thermal energy is removed from the cold side through forced liquid flow. The mass flow rate of the water/glycol mixture is measured as 17 g/s and the coolant mixture heat capacity is 3.89 J/gK. The convection coefficient was determined empirically and is 1400 W/m^2 K. Heat losses from the hot block (which is insulated with glass-fibre) are included in the simulation as described in [28]. The time step size used for the simulation is 3 s. This choice is based on the fact that the test rig is able to vary the temperature difference at a maximum rate of 0.2 K/s, therefore a time step of 3 s ensures that the temperatures of the thermal masses do not change much and at the same time guarantees a good evolution of the transient solution provided by the heat equation.

The TEG module used is manufactured by European Thermodynamics Ltd. (model code: GM250-127-14-10) and has an open-circuit thermal conductivity $k = 1.62$ W/mK, surface

$A = 1600\ \text{mm}^2$, thickness $L = 3$ mm, thermal diffusivity $\epsilon = 1e^{-6}\ \text{m}^2/\text{s}$.

Electrical characterisation of the module used was performed at two different temperature differences, $\Delta T = 50\ ^\circ\text{C}$ and $\Delta T = 150\ ^\circ\text{C}$, both with a mechanical force of 2000 N on the module, corresponding to a pressure of 1.2 MPa. Results obtained are shown is Fig. 4. These data are then used to obtain the coefficients of Eq. (14): $m_{V_{OC}} = 0.048; m_{R_{int}} = 0.0045; q_{R_{int}} = 1.52$.

4.2. Comparison and discussion of results

The designed transient lasts for 55.5 min and is intended to produce several power and load steps. The VEE program records all the electrical data, temperatures, mechanical pressure and time. The transient parameters are as follows, where P_{in} is the DC electrical power to the heater and I_{load} is the current value set in the electronic load:

1. $P_{in} = 50$ W; $I_{load} = 0$ A (open-circuit) @ time = 0 s.
2. $P_{in} = 50$ W; $I_{load} = 0.2, 0.4, 0.6, 0.8, 1$ A @ time = 1195, 1210, 1229, 1247, 1286 s.
3. $P_{in} = 150$ W; $I_{load} = 1$ A @ time = 1286 s.
4. $P_{in} = 150W$; $I_{load} = 1.2, 1.4, 1.6, 1.4, 1.2, 1.0, 0.8, 0.6$ A @ time = 2761, 2780, 2795, 2828, 2844, 2877, 2946, 3109 s.

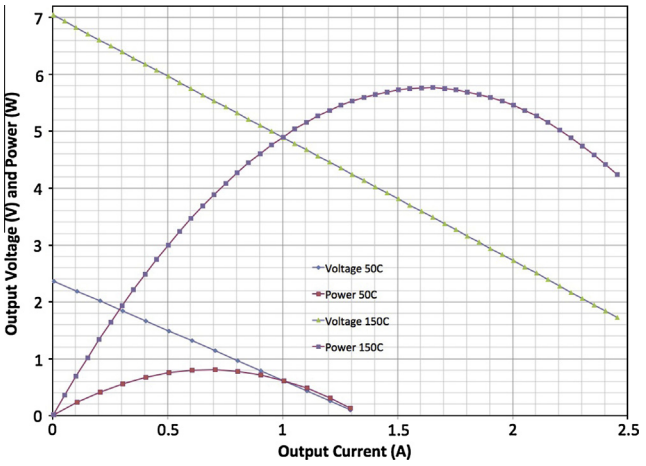

Fig. 4. Electrical characteristic of the TEG module used in the experiment, for two different temperature gradients $\Delta T = 50, 150\ ^\circ\text{C}$, clamped at 2 kN/1.2 MPa.

This experiment is designed to test the simulation model under thermal and electrical transients of difference magnitude. Different temperature variation rates were applied both in open-circuit and at-load, with several electrical load steps. The Simulink program runs without interruptions, therefore testing it under different thermal and electrical conditions ensures that there are no offsets that would make the results valid for just one of those operating conditions.

Fig. 5 shows both the experimental and simulation results in the same graph, for comparison. In particular the temperature difference and the output electrical power are plotted versus the transient time. During the transient the temperature difference across the TEG device varies from 5 °C to almost 150 °C, leading to some thermal expansion effects in the whole system. The mechanical pressure on the system could not be controlled during the test, but active control of the clamping force will be incorporated into a future test rig to compensate for thermo-mechanical effects. In previous work [28] it was noted that different pressure loads slightly influence the contact resistances in the system, thus affecting the thermal conductivity and the power produced by the TEG module. Their effect should not account for more than a 5% change in the results.

As it can be appreciated from Fig. 5, there is no delay in the response of the simulated results with respect to the experimental data. The simulation results show very good agreement with the experimental results, accurately tracking the electro-thermal coupled effects occurring in the TE system. The Root Mean Square Error (RMSE) is 3.58 °C for the temperature difference and 0.2 W for the power output. The RMSEs normalised to the values range (NRMSE) become 2.76% and 4.55% for the temperature difference and the output power, respectively. There are no works in the literature that proposed a simulation model for TEG systems demonstrating similar prediction performance under varying thermal and electrical conditions as the one presented in this article. As a consequence it is difficult to compare the data presented here to other simulation results reported in the literature.

It is very interesting to note the close effect that the load current has on the temperature gradient across the device. Every increase in I_{load} leads to a decrease in temperature due to the greater value of the Peltier term of Eq. (9). Conversely, the last 500 s of the test show that a smaller load current increases the rate of change of temperature. The effective thermal conductivity of the TEG module varies markedly, depending on the current flowing through the module. MPPT converters should take this thermal

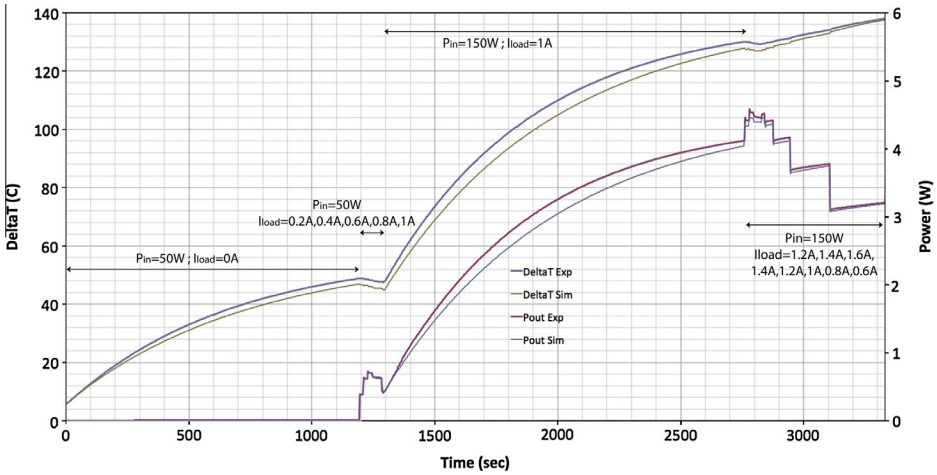

Fig. 5. Experimental and simulated transient results showing the temperature difference and the output electrical power versus the time.

variation into account when setting the optimum operating point for maximum efficiency or power generation.

Future work will develop a model of the system that incorporates the non-linear effects introduces by a MPPT converter. The model will be adapted to a typical waste heat energy recovery system from exhaust gas for automotive applications.

5. Conclusion

This paper presents an innovative and powerful computer tool to accurately simulate real thermoelectric power generating systems even during transient conditions. The proposed simulation program, designed in Simulink–Matlab, deals with all the most important thermoelectric effects and is able to cope with both thermal and electrical dynamics. Consequently it can greatly help the design phase of large-scale and/or complicated thermoelectric systems.

A comparison of experimental and simulation results shows the accuracy and capability of the model, showing that it can be employed to study transients and steady-state operation of real TE systems with confidence.

Acknowledgements

The authors would like to thank Dr. Steven Roper and Dr. James Buckle of the University of Glasgow for their contribution to the project and Mr. Peter Miller and the mechanical workshop of the University of Glasgow for their work in creating the test rig used for the experiments.

References

[1] Du C-Y, Wen C-D. Experimental investigation and numerical analysis for one-stage thermoelectric cooler considering Thomson effect. Int J Heat Mass Transfer 2011;54:4875–84.
[2] Lazard M. Heat transfer in thermoelectricity: modelling, optimization and design. In: 7th IASME/WSEAS international international conference on heat transfer, thermal engineering and environment. p. 129–34.
[3] Chen J, Yan Z, Wu L. The influence of Thomson effect on the maximum power output and maximum efficiency of a thermoelectric generator. J Appl Phys 1996;79:8823.
[4] Min G, Rowe DM, Kontostavlakis K. Thermoelectric figure-of-merit under large temperature differences. J Phys D: Appl Phys 2004;37:1301–4.
[5] Riffat S, Ma X. Thermoelectrics: a review of present and potential applications. Appl Therm Eng 2003;23:913–35.
[6] Siviter J, Knox A, Buckle J, Montecucco A, McCulloch E. Megawatt scale energy recovery in the Rannkine cycle. In: Energy conversion congress and exposition (ECCE). IEEE; 2012. p. 1374–9.
[7] Crane D, LaGrandeur J, Ranalli M, Adldinger M, Poliquin E, Dean J, et al. TEG on-vehicle performance and model validation and what it means for further TEG development. In: International conference on thermoelectrics (ICT'12).
[8] Risse S, Zellbeck H. Close-coupled exhaust gas energy recovery in a gasoline engine. Res Therm Manage 2013;74:54–61.
[9] Wang Y, Dai C, Wang S. Theoretical analysis of a thermoelectric generator using exhaust gas of vehicles as heat source. Appl Energy 2013;112:1171–80.
[10] Patyk A. Thermoelectric generators for efficiency improvement of power generation by motor generators environmental and economic perspectives. Appl Energy 2013;102:1448–57.
[11] Champier D, Bédécarrats J, Kousksou T, Rivaletto M, Strub F, Pignolet P. Study of a TE (thermoelectric) generator incorporated in a multifunction wood stove. Energy 2011;36:1518–26.
[12] OShaughnessy S, Deasy M, Kinsella C, Doyle J, Robinson A. Small scale electricity generation from a portable biomass cookstove: prototype design and preliminary results. Appl Energy 2013;102:374–85.
[13] Suter C, Jovanovic Z, Steinfeld A. A 1 kWe thermoelectric stack for geothermal power generation modeling and geometrical optimization. Appl Energy 2012;99:379–85.
[14] Sark WV. Feasibility of photovoltaic thermoelectric hybrid modules. Appl Energy 2011;88:2785–90.
[15] Xiao J, Yang T, Li P, Zhai P, Zhang Q. Thermal design and management for performance optimization of solar thermoelectric generator. Appl Energy 2012;93:33–8.
[16] Qiu K, Hayden aCS. Development of a novel cascading TPV and TE power generation system. Appl Energy 2012;91:304–8.
[17] Biswas K, He J, Blum ID, Wu C-I, Hogan TP, Seidman DN, et al. High-performance bulk thermoelectrics with all-scale hierarchical architectures. Nature 2012;489:414–8.
[18] Zebarjadi M, Esfarjani K, Dresselhaus MS, Ren ZF, Chen G. Perspectives on thermoelectrics: from fundamentals to device applications. Energy Environ Sci 2012;5:5147.
[19] Lineykin S, Ben-Yaakov S. Modeling and analysis of thermoelectric modules. IEEE Trans Indust Appl 2007;43:505–12.
[20] Chen M, Rosendahl LA, Condra TJ, Pedersen JK. Numerical modeling of thermoelectric generators with varing material properties in a circuit simulator. IEEE Trans Energy Convers 2009;24:112–24.
[21] Naji M, Alata M, Al-Nimr MA. Transient behaviour of a thermoelectric device. Proc Inst Mech Eng Part A: J Power Energy 2003;217:615–21.
[22] Cheng C-H, Huang S-Y. Development of a non-uniform-current model for predicting transient thermal behavior of thermoelectric coolers. Appl Energy 2012;100:326–35.
[23] Meng J-H, Wang X-D, Zhang X-X. Transient modeling and dynamic characteristics of thermoelectric cooler. Appl Energy 2013;108:340–8.
[24] Montecucco A, Buckle JR, Knox AR. Solution to the 1-D unsteady heat conduction equation with internal Joule heat generation for thermoelectric devices. Appl Therm Eng 2012;35:177–84.
[25] Lee H. Optimal design of thermoelectric devices with dimensional analysis. Appl Energy 2013;106:79–88.
[26] Chen L, Cao D, Yi H, Peng FZ. Modeling and power conditioning for thermoelectric generation. In: IEEE power electronics specialists conference. IEEE; 2008. p. 1098–103.
[27] Woo BC, Lee DY, Lee HW, K IJ. Characteristic of maximum power with temperature difference for thermoelectric generator. In: 20th International conference on thermoelectrics; 2001. p. 431–4.
[28] Montecucco A, Buckle J, Siviter J, Knox AR. A new test rig for accurate nonparametric measurement and characterization of thermoelectric generators. J Electron Mater 2013;42(7):1966–73.
[29] Montecucco A, Siviter J, Knox A. Simple, fast and accurate maximum power point tracking converter for thermoelectric generators. In: Energy conversion congress and exposition (ECCE). IEEE; 2012. p. 2777–83.